

WALKER DEPARTMENT OF MECHANICAL ENGINEERING
Nuclear Engineering Teaching Laboratory

Pickle Research Campus R-9000 • Austin, Texas 78758 • 512-232-5380 • FAX 512-471-4589
nuclear.engr.utexas.edu • wcharlton@austin.utexas.edu

March 31, 2020

ATTN: Document Control Desk
U. S. Nuclear Regulatory Commission
Washington, D.C. 20555-0001

Geoffrey Wertz, P.E.
Non-Power Production and Utilization Facility Licensing Branch
Division of Advance Reactors and Non-Power Utilization
Nuclear Reactor Regulation

SUBJECT: Docket No. 50-602, Facility Operating License R-129 - Submission of Neutronic and Thermal Hydraulic Analysis for the University of Texas at Austin Research Reactor

REFERENCE: October 18, 2018 letter: University- of Texas at Austin - Summary of Site Visit and Request for Schedule for Completion of the Reactor Analyses RE: Renewal of Facility Operating License No. R-129 for The University of Texas at Austin Research Reactor (EPID NO. L-2017-RNW -0032)

Sir:

We respectfully submit neutronics and thermal-hydraulic analysis, attached. If you have any questions, please contact me at 512-232-5373 or whaley@mail.utexas.edu.

P. M. Whaley

A handwritten signature in cursive script, appearing to read "P. M. Whaley".

I declare under penalty of perjury that the foregoing is true and correct.

A handwritten signature in cursive script, appearing to read "W. S. Charlton".

W. S. Charlton

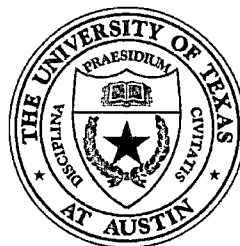
ATT:

- (1) Analysis of the Neutronic Behavior of the Nuclear Engineering Teaching Laboratory at the University of Texas
- (2) Thermal Hydraulic Analysis of the University of Texas (UT) TRIGA Reactor

AD20
NRR

**THERMAL HYDRAULIC ANALYSIS OF
THE UNIVERSITY OF TEXAS (UT) TRIGA REACTOR**

Paul (Michael) Whaley and William S. Charlton
Nuclear Engineering Teaching Laboratory
University of Texas at Austin
Austin, TX 78758



March 31, 2020

1.0 INTRODUCTION

This report documents analysis of the thermal hydraulic characteristics of the UT TRIGA nuclear research reactor in support of renewal of the U.S. Nuclear Regulatory Commission facility operating license. NRC guidance¹ specifies definition of a limiting core configuration (LCC) as the core that would yield the highest power density using the fuel specified for the reactor, with all other core configurations encompassed by safety analysis for the LCC. Coupled analyses for neutronic and thermal hydraulic behavior are used to characterize thermal hydraulic performance of the LCC. This report describes the thermal hydraulic analysis, the neutronic analysis is a separate report².

Heat generated by fission in operation of the UT TRIGA reactor is transferred by conduction from the fuel to the cladding. The fuel cladding is the principal safety feature of the TRIGA reactor, preventing radioactive fission products from release that could result in possible hazardous exposure to radiation for facility personnel and the general public. The integrity of the fuel cladding is assured if the fuel temperature remains below specific values (830°C during pulsing³, 950°C if the cladding temperature is less than 500°C, and 1150°C if the cladding temperature is above 500°C⁴).

Heat is transferred to water [or air in the case of a loss of coolant accident (LOCA)] surrounding the fuel element cladding. The cooling medium temperature increase develops buoyancy forces that drive convection flow. Cooling flow is impeded by momentum changes and friction (across the grid plates, fuel element end fittings, and fuel element cladding surfaces). Above a "critical" heat flux (CHF), cooling flow may not be adequate to prevent exceeding the temperature limits, and 'burnout' will occur. The NRC guidance limits the ratio of heat flux to critical heat flux (CHFR) to a value greater than 2.0. A correlation for CHFR applicable to TRIGA reactors has been developed by Bernath⁵ and is used in this analysis.

The fuel element in the LCC that operates closest to the limits is the element generating the most power, 'hot channel. Analysis of the hot channel demonstrates that operation at the maximum licensed power level and within licensed reactivity limits maintains the reactor fuel below the temperature limits, and heat transfer to the surrounding cooling media remains above the CHFR limit.

TRACE (TRAC/RELAP Advanced Computational Engine) is the NRC's flagship thermal-hydraulics analysis tool consolidating and extending the capabilities of NRC's three legacy safety codes: TRAC-P, TRAC-B and RELAP. These codes are designed to perform best-estimate analyses of operational transients and accident scenarios by modeling physical geometry and thermodynamic conditions. TRACE and RELAP were developed for commercial nuclear reactors applications, and RELAP has also been widely used in characterizing non-power/research reactor thermal hydraulic performance.

Thermal hydraulic modeling of the hot channel in the UT TRIGA reactor was performed using TRACE. The model was developed using standard, classical methods applied to the fuel element geometry and fuel element pitch. However, fuel element construction includes complex end fittings not well represented in modeling flow resistance classically, and coefficients characterizing the resistance to cooling flow for the UT

¹ NURGE 1537, *Guidelines for Preparing and Reviewing Applications for the Licensing of Non-Power Reactors, Format and Content*

² Analysis of the Neutronic Behavior of the Nuclear Engineering Teaching Laboratory at The University of Texas, Radiation Center – Oregon State University

³ TRD-070-0.1006.05 Rev A, *Pulsing Temperature Limit for TRIGA Fuel* (TRIGA Reactors Division of General Atomics-ESI, 2008)

⁴ NUREG/CR-2387 *Credible Accident Analyses for TRIGA and TRIGA-Fueled Reactors* (PNL-4028, April 1962)

⁵ ANL RETR TM 07 01, *Fundamental Approach to TRIGA Steady-State Thermal-Hydraulic CHF Analysis*, E. E. Feldman (2007)

TRIGA were therefore developed in the computational fluid dynamics code FLUENT.⁶ Data in TRACE output files were parsed to identify maximum fuel temperature and variables used in the Bernath correlation.

TRACE has an internal library of standard material properties relevant to power reactors. The library does not include properties for zirconium and TRIGA fuel; these material characteristics are supplied as manual input. The ratio of the maximum power in the hot channel to average core-wide element power (peaking factor, developed from the neutronics analysis) is used to extend transient calculations from elements generating core average power to calculations for the element generating the maximum power in the core. An estimate of the prompt neutron lifetime was generated in an MCNP adjoint calculation to support reactivity calculations in TRACE.

An auxiliary program distributed with MCNP (MAKXS) was used to generate neutron interaction cross sections at specific fuel and water temperatures. These cross sections were used in MCNP criticality calculations to develop reactivity temperature-coefficients for TRACE reactivity calculations. The MCNP model developed in the neutronics analysis was used to generate delayed neutron precursor constants. The constants were used to develop time-dependent heat generation from fission following shutdown for LOCA analysis. The heat generation from fission product decay for LOCA analysis was developed from the method described in ANSI/ANS-5.1-2014, Decay Heat Power in Light Water Reactors. Heat generated from neutron interaction with fission products was neglected.

Analyses were developed to characterize performance associated with steady-state operation, reactor pulsing, continuous control rod withdrawal transients, and a LOCA. Validation of the modeling was performed by comparing analytic results to peak temperatures during steady state operations, and power levels and temperatures that occurred during pulsing operation. The model was validated and then used to develop the LCC.

2.0 TRACE MODEL

The TRACE model uses 'break' elements that establish pressure and temperature fluid boundary conditions. Pool water is delivered from break through a 'downcomer' with a horizontal structure connecting the downcomer to the inlet of the fuel element flow channel. The fuel element flow channel discharges to another break. A conceptual diagram of the model is provided in Fig. 1.

2.1 Flow Channel Geometry

The cooling flow channel is modeled as a heated pipe with thermodynamic characteristics based on physical dimensions and properties of the coolant surrounding the fuel elements. The outer diameter of a fuel element (D_F) is 1.475 in. The outer diameter of the fuel is 1.435 in. with an inner diameter of 0.25 in. filled with a 0.225 in. diameter zirconium rod. The cladding is 0.020 in. thick, with a small gap between the inner cladding diameter and the fuel outer diameter. The center-to-center distance to adjacent elements (pitch, P_e) is 1.714 in.

⁶ (Doctoral Dissertation) Development of thermal Hydraulic Correlations for the University of Texas at Austin TRIGA Reactor Using Computational Fluid Dynamics and In-Core measurements, A. D. Brand (2013), <https://repositories.lib.utexas.edu/handle/2152/23039>

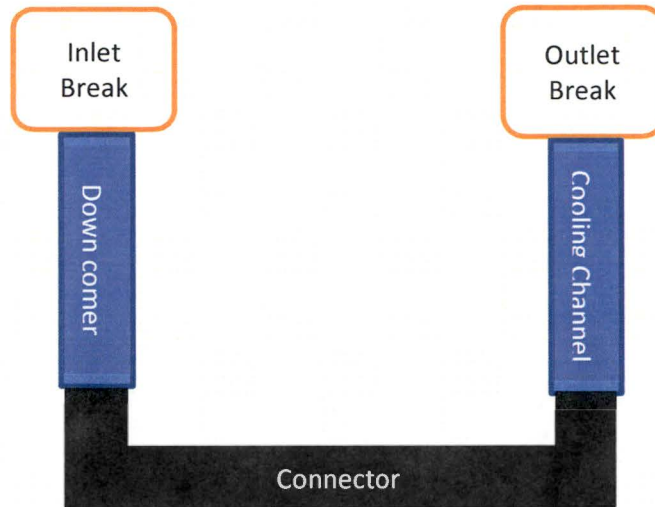


Figure 1: UT TRACE Model

The geometry of the fuel element and surrounding flow area (Figs. 2 and 3) is modeled as a hexagon with an inner radius (i.e., the largest circle centered in and bounded by the hexagon) of $\frac{1}{2}$ of the pitch. A large fraction of the model is occupied by the fuel element, leaving a relatively small flow area. End fittings have more complex geometry and are approximated using hydrodynamic characteristics.

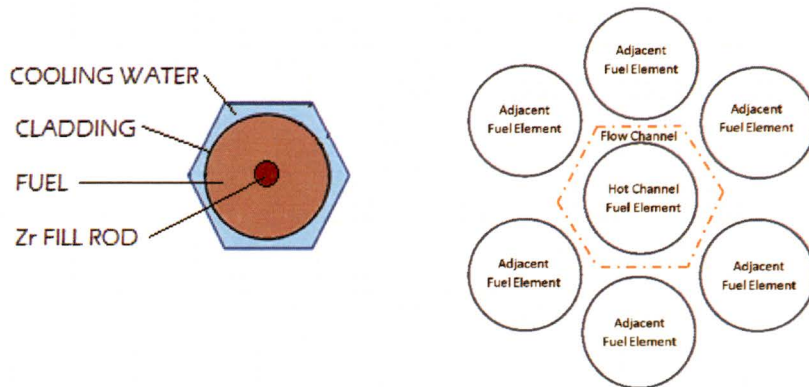


Figure 2: Flow Channel for UT TRIGA

The area of the flow channel (A) is the area of the hexagon less the area of a fuel element. Using p_e as pitch and D_F as the diameter of the fuel element, the area of the flow channel is given by:

$$A = \frac{\sqrt{3}}{2} \cdot p_e^2 - \pi \cdot \left(\frac{D_F}{2}\right)^2 \quad \text{Eqn 1}$$

The wetted perimeter (P_w) is the perimeter of the fuel element:

$$P_w = \pi \cdot D_F \quad \text{Eqn 2}$$

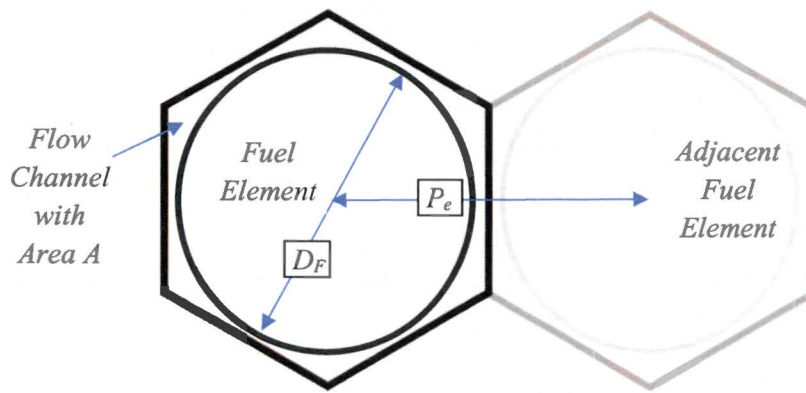


Figure 3: Pitch and Fuel Element Diameter And Relation to Flow Channel

Non-circular pipes are approximated from the flow area and the wetted perimeter (P_w) with an equivalent hydraulic diameter (D_h) calculated using:

$$D_h = \frac{4 \cdot A}{P_w} \quad \text{Eqn 3}$$

Substituting equations 1 and 2 into equation 3 yields the following for the hydraulic diameter:

$$D_h = \frac{4}{\pi \cdot D_F} \cdot \left[\frac{\sqrt{3}}{2} \cdot P_e^2 - \pi \cdot \left(\frac{D_F}{2} \right)^2 \right] = \frac{2 \cdot \sqrt{3}}{\pi} \cdot \frac{P_e^2}{D_F} - D_F = D_F \cdot \left[\frac{\sqrt{3}}{2} \cdot \frac{P_e^2}{D_F^2} - 1 \right] \quad \text{Eqn 4}$$

Equations 1-4 are used the TRACE modeling.

2.2 Thermal Hydraulic Loss Factors

Pressure drops (head loss) across hydraulic components are the product of the fluid flow and factors such as the coefficient of friction between the fluid and the pipe wall, changes in flow area and diameter, flow channel surface roughness, and/or flow channel length. Standard practice defines the characteristics that determine head loss as coefficients, or K factors based on experimentally derived correlations to support conservation of energy and momentum calculations for fluid flow. The surface roughness for TRIGA fuel elements is $6.998E-6$ ft.⁷ Correlation of K factors with geometry and flow are based on historical, experimental measurements with cylindrical pipes. Additional work extended this to rectangular ducts; non-circular cross sections are reduced to a flow area and hydraulic diameter developed as circular geometry. These correlations apply after flow is fully developed following geometry perturbations that create turbulence. The geometry inherent in TRIGA fuel challenges application of standard formula to calculate the K factors:

- The actual entrance and exit to the flow channel between the grid plates is directed by fins, a center pin, and a conical shape with part of the structure extending into the volume bounded by grid plate penetrations; the wetted perimeters vary continuously from entrance to exit for each end fitting.
- The fuel element end fittings are partially inserted in grid plate penetrations that fix the position of

⁷ Oregon State University, Model Editor File for the OSTR thermal hydraulic Model (private communication)

the fuel elements in the core, causing area expansion and contraction over parts of the end fittings at the entrance and exit of the upper and lower grid plates.

- The interface between adjacent fuel channels is not separated by a physical boundary, and differential pressure between adjacent flow channels can support cross-channel flow, although analysis has shown that any cross-flow is small and has “no effect on fuel temperature” with a slight increase in critical heat flux ratio⁸; cross flow is neglected in this analysis.

Therefore, thermal hydraulic analysis to support relicensing was developed to independently model thermal hydraulic performance at the end fittings from (1) first principles, (2) the TRACE thermal hydraulics code, and (3) the FLUENT computational fluid dynamics code. The results of experiments in the TRIGA core were used to evaluate UT TRIGA-specific K factors based on actual fuel element geometry. The values determined from the UT research program (Table 1) were used in modeling for TRACE calculations.

Table 1: UT TRIGA Specific K Factors

APPLICATION	K Factor
TRIGA Lower Channel	1.63
TRIGA Upper Channel	1.12

2.3 Hydrostatic Pressure

The cooling pressure and temperature specifications in the break components are based on local environmental conditions (barometric pressure, confinement pressure regulation) and the pool (level and water temperature). The NETL building is approximately 240 m above sea level, and the reactor bay confinement system is designed to control differential pressure to 0.06 in. below atmospheric pressure (minimal compared to atmospheric pressure). Total pressure at the top of the core is:

$$p_T = 96\{KPa\} + p_{H_2O} \quad \text{Eqn 5}$$

Pool water is nominally 7.25 m, with a minimum of 5.25 m above the core. Pool water temperature is nominally 25-27 °C, and limited to less than 49 °C. Where g denotes the gravitational constant ($9.8 \text{ m}\cdot\text{s}^{-2}$), the pressure (p_{H_2O}) exerted by a column of water (at density ρ in $\text{kg}\cdot\text{m}^{-3}$ and height h in m) is given by:

$$p_{H_2O} = \rho \cdot g \cdot h \quad \text{Eqn 6}$$

A break is also connected to the exit of the core, representing exit from the flow channel to the same parameters as the entrance. Pressure boundary conditions for the limiting cases are provided in Table 2, converted to British units for TRACE input.

Table 2: LCC Temperature & Pressure

Condition	Temp (°F)	Pressure (Psia)
Limiting	120.2	21.3
Nominal	77	24.2

⁸ Armed Forces Radiobiology Research Institute (AFRRI) submittal of Safety Analysis Chapters 4 and 13 to the USNRC (ML101650422, submitted on March 4, 2010)

2.4 Heat Structure Modeling

The heated length of the fuel element is modeled as a TRACE heat structure. Heat structure cells simulate the zirconium fill rod at the center of the fuel element, the fuel matrix, the gap between the fuel and cladding, and the cladding. The UT TRIGA heat structure consists of 15 axial cells that transmit heat from the fuel element to the cooling channel. The UT TRIGA model uses a gas gap heat transfer coefficient⁹ of 500 Btu h⁻¹ ft⁻² °F⁻¹, (2840 W m⁻² K⁻¹). The flow channel includes non-heated lengths that are not part of the heat structure above and below the heated length representing integral graphite reflector and end fittings (with a space in the upper end fitting for fission gas collection incorporated above the upper graphite reflector).

2.5 Power/Reactivity Application

Fuel element power is used as an input for steady-state and LOCA analysis, and it supports cases with time-dependent reactivity variation. Reactivity is used as an input for transient analysis (pulsing and control rod withdrawal transient analyses). Reactivity transients are used to generate power levels at times for a fuel element representing the core average in pulsing and control rod withdrawal analysis; then the time dependent average element power level is scaled by the core peaking factor to represent the hot channel in a time dependent power calculation. For LOCA analysis, the time dependent behavior of power following shutdown was evaluated and developed using reactor kinetics for fission power and for decay heat from fission product using the method of ANSI/ANS-5.1-2014 (equation 7 and 8). For an irradiation interval of time T , a decay time of t , and irradiation intervals i and a constant fission rate of unity, decay heat power (F , units of MeV/fission) can be represented analytically as a function using analytic fit constants α and β (the fit constants are provided for all 23 components in the standard):

$$F_i(t, T_a) = \sum_{j=1}^{23} \frac{\alpha_{i,j}}{\lambda_{i,j}} \cdot \exp(-\lambda_{i,j} \cdot t) \cdot [1 - \exp(-\lambda_{i,j} \cdot T)] \quad \text{Eqn 7}$$

Assuming a single power generation interval and a long operating time, this reduces to:

$$F(t) = \sum_{j=1}^{23} \frac{\alpha_j}{\lambda_j} \cdot \exp(-\lambda_j \cdot t) \quad \text{Eqn 8}$$

The ratio of decay heat power to initial reactor power depends on a reactor specific energy generation per fission (MeV/fission) that is also used in TRACE transient calculations. The MCNP burnup analysis output tabulates fission energy yield data (Q value, Table 3) as given in Table 3.

Table 3: Fission Energy Yield
from MCNP Analysis

Nuclide	Q-Value (MeV)
92235	180.88
92238	181.31
94239	189.44
94241	188.99

⁹ The University of Texas Safety Analysis Report, Revision 1.01 (5/91)

The fraction of energy produced by each fissionable material (Table 4) is taken from an MCNP burnup calculation supporting the neutronics report for use in TRACE analysis. Estimates of the fraction of isotope 92235 fissions at greater than thermal energy are assumed to have Q values consistent with isotope 92238.

Table 4: Fission Isotope Nuclear Characteristics¹⁰

Nuclide	Fraction	Fission		Fissions at Energy
		Cross-section (b)	Energy Range	
92235	19.8%	585.1	<0.625 eV	94.28%
		274.4	0.625 eV – 100 keV	4.99%
92238	80.2%	1.241	>100 keV	0.72%
		0.03064		

The kinetics treatment used fission product nuclear characteristics (precursor fractions, decay constants, and the generation time) from MCNP adjoint calculations given in Table 5. Thermal/non-thermal fission fractions are taken from the MCNP burnup calculations.

Table 5: Delayed Neutron Precursor Group Characteristics

	β_i	Standard Deviation	Energy (MeV)	Standard Deviation	λ_i (s ⁻¹)	Standard Deviation	T _{1/2} (s)	Standard Deviation
1	0.00022	0.00005	0.40605	0.00460	0.01334	0.00000	51.960	0.004
2	0.00138	0.00013	0.47218	0.00202	0.03273	0.00000	21.178	0.001
3	0.00138	0.00012	0.44217	0.00202	0.12080	0.00000	5.73797	0.00005
4	0.00296	0.00019	0.55867	0.00181	0.30295	0.00001	2.28799	0.00008
5	0.00113	0.00011	0.51895	0.00294	0.85032	0.00004	0.81516	0.00004
6	0.00059	0.00009	0.53926	0.00495	2.85537	0.00021	0.24227	0.00002

Heat generation distribution in the heat structure is based on mesh tally calculations from MCNP modeling described in the neutronics report. The mesh tally provides average fission density at 225 locations throughout the fuel rod. These 225 locations consist of equal volume segments of the fuel with 15 radial segments and 15 axial segments. The normalized mesh values were applied to locations in TRACE. Equal volume segments were allow direct averaging of temperatures in the fuel. This 15x15 matrix was used as a power distribution profile in TRACE.

MCNP calculations were used to acquire estimates of the prompt neutron generation time and effective delayed neutron fractions. The MCNP calculations produced an estimated prompt-neutron generation time of 43.81±0.53 μs (Table 6). The 1992 Safety Analysis Report for the UT TRIGA cited a prompt generation time of 41 μs, which is consistent with that calculated by MCNP. For the purposes of this report the MCNP calculated value was considered to be more applicable since it utilized current parameters.

The effective delayed neutron fraction has historically been used as 0.007 for the UT TRIGA. The MCNP calculated value for β_{eff} was 0.00737±0.00006 (Table 6). Calculating pulsing reactivity in units of \$ based on β_{eff} of 0.007, and therefore represents 91% of the nominal pulsed reactivity. Data from two series of reactor pulses with varying reactivities were analyzed using the Fuchs-Hansen pulse model modified to evaluate β_{eff}

¹⁰ <https://www.ndc.jaea.go.jp>, Fission at Energy from MCNP burnup calculation

from the convergence of iterative calculations. Pulses from November 2018 were found to have a β_{eff} of 0.007306, and from March 2020 to have a β_{eff} of 0.007382. Therefore, a correction is necessary in model validation against historical data.

Table 6: MCNP Calculated Reactivity Parameters

Parameter	Estimate	Standard Deviation
Generation Time	43.81 μs	0.53 μs
β_{eff}	0.00737	0.00006

2.6 User Defined Materials

Zirconium properties are provided in Table 7. The zirconium fill rod is slightly smaller than the center hole of the fuel element. Therefore, the standard zirconium density was reduced by the ratio of the zirconium rod volume to the whole volume.

Table 7: Zirconium Properties

Temperature °F	Density lbm/ft ³	Heat Capacity (C_p) Btu/lbm-°F	Thermal Conductivity Btu/h-ft-°F	Emissivity
-99.4	328.18	0.082284	14.562	0.8
260.6	328.18	0.102199	12.4812	0.8
620.6	328.18	0.122114	11.9592	0.8
980.6	328.18	0.142029	12.4812	0.8
1340.6	328.18	0.161943	13.6944	0.8
1700.6	328.18	0.181858	15.0228	0.8
2240.6	328.18	0.211731	16.6392	0.8
4481.2	328.18	0.335679	21.6392	0.8

Reference values¹¹ for specific heat capacity (C_p) and thermal conductivity (k_c) of TRIGA fuel are:

- $C_p = 0.018 \pm 0.009$ watts [$\text{cm}^{-1} \text{°C}^{-1}$]
- $k_c = 2.04 + 0.00417 \times T$ [$\text{W s}^{-1} \text{cm}^{-3} \text{°C}^{-1}$] (note that this is given as a function of material temperature T)

These formulae were converted to British units and used to generate tabular values (Table 8) for TRACE.

¹¹ E-117-833, The U-Zr_x Alloy: Its Properties and Use in TRIGA Fuel (Simnad, General Atomics Project No. 4314)

Table 8: Uranium-Zirconium Hydride (Fuel)

Temperature °F	Density lbm/ft ³	Heat Capacity (Cp) Btu/lbm-°F	Thermal Conductivity Btu/h-ft-°F	Emissivity
-65.6	374.5	0.029754	10.16021	0.8
294.4	374.5	0.091403	10.16021	0.8
654.4	374.5	0.153051	10.16021	0.8
1014.4	374.5	0.2147	10.16021	0.8
1374.4	374.5	0.276349	10.16021	0.8
1734.4	374.5	0.337997	10.16021	0.8
2274.4	374.5	0.43047	10.16021	0.8
4548.8	374.5	0.814165	10.16021	0.8

2.7 Temperature Feedback

Temperature feedback is incorporated in the transient analysis for pulsing and control rod withdrawal events. General Atomics¹² indicates that the fuel temperature coefficient (water reflected) is convex, with a minimum occurring about 300°C. An analysis at AFRRRI¹³ based on DIF3D (Argonne National Laboratory, diffusion and transport theory code) calculations show convex structure from 10-1000°C for TRIGA fuel. Standard MCNP cross sections are available in intervals of about 300°C; it is not possible to get data from calculations where cross-sections are separated by 300°C that would provide accurate data for derivation of cross sections. Therefore, an auxiliary code distributed with MCNP (MAKXSF) was used to generate data over the range for operations of interest. Although fuel temperature and water temperature coefficients are generally considered independently, they are coupled. The temperatures used for generating these cross sections are shown in Table 9.

Table 9: Cross Section Temperatures (°F)

Fuel	98.33	118.13	344.93	458.33	571.73	841.73	1111.73	1291.73	1471.73	1651.73
Water	76.73	76.73	80.33	107.33	134.33	168.53	188.33	215.33		

Criticality calculations with the MCNP model developed in the neutronics analysis were performed using all permutations of temperatures indicated. Fuel temperature, water temperature, and the associated excess reactivity for each calculation was used to generate a function of the two temperatures. The function was used to evaluate values ½ degree above and ½ degree below specific fuel temperatures with water temperature held constant, and then varying water temperature with constant fuel temperatures. The results are provided graphically at selected fuel temperatures, fuel temperature reactivity coefficients for a series of constant moderator temperatures (Fig. 4) and moderator temperature coefficients for a series of constant fuel temperatures (Fig. 5).

¹² Simnad op. cit.

¹³ AFRRRI op. cit.

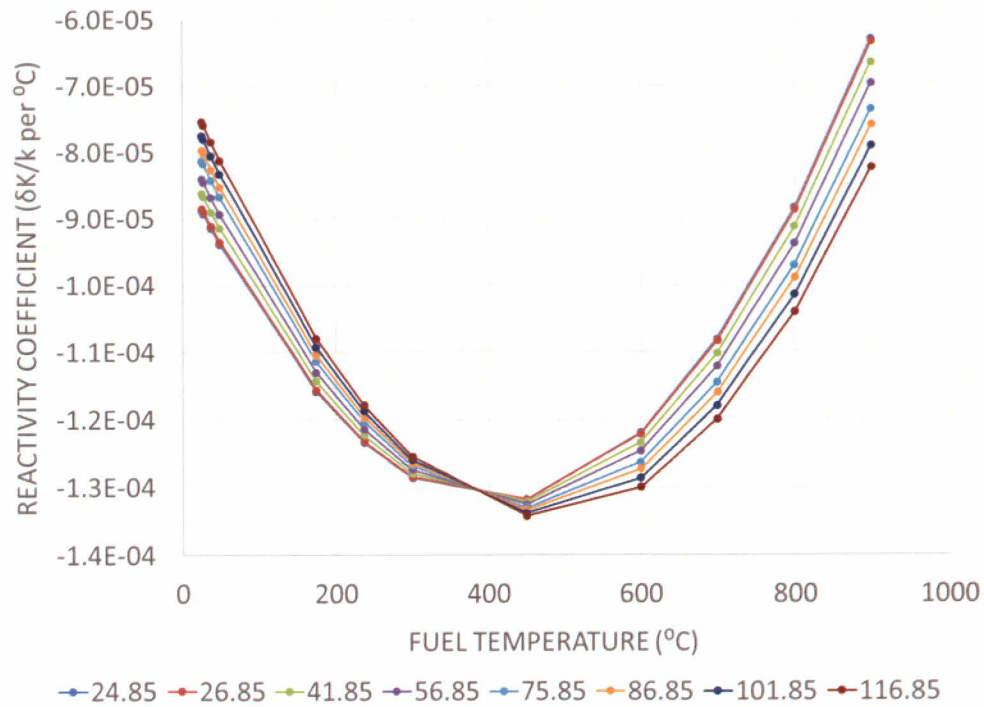


Figure 4: Temperature Coefficient of Reactivity for the Fuel Versus Fuel Temperature (shown at a variety of fixed coolant temperatures)

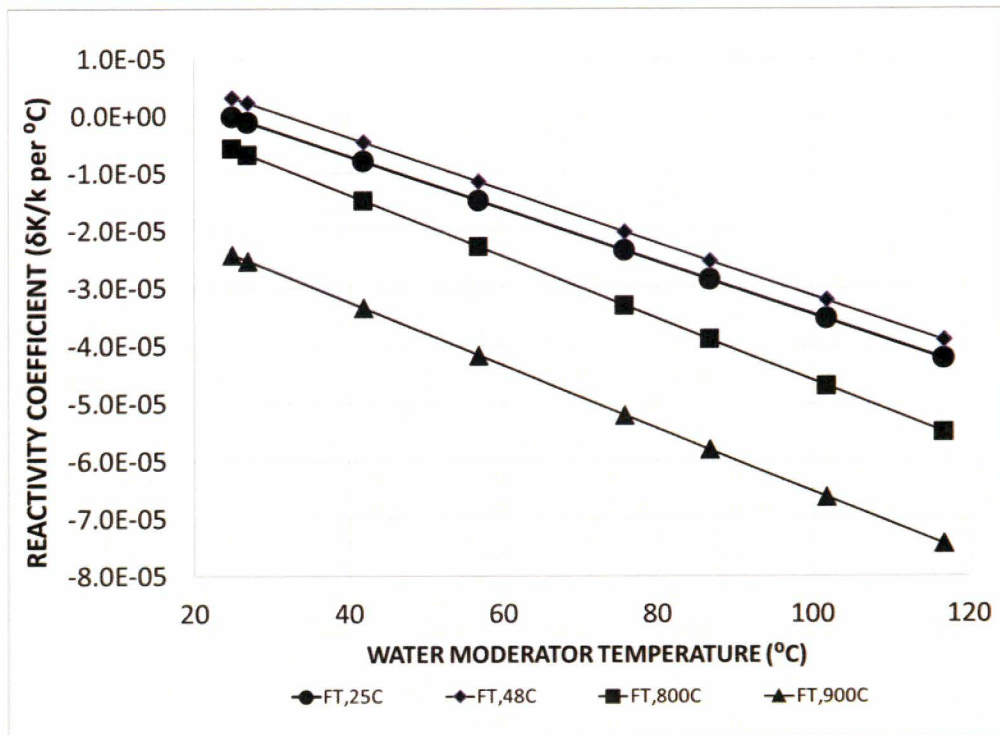


Figure 5: Water Temperature Coefficient of Reactivity Versus Water Moderator Temperature (shown at a variety of fixed fuel temperatures)

The maximum variation in the fuel temperature reactivity coefficient at low temperature (with respect to water temperature) is on the order of 10% from nominal water temperature to temperatures near boiling in the core. The water temperature change is dominated by the decrease in water density as temperature increases; lower water density increases scattering length and reduces moderation in the cooling channels. As fuel temperature increases there is less absorption in the fuel matrix and consequently more neutron scattering out of the fuel matrix into the water. These competing effects cause the difference with respect to water temperature to converge and then reverse the difference at higher fuel temperatures where the neutron spectrum is hardened in the fuel to shift moderation to the water region. With a constant fuel temperature, the moderator temperature coefficient change is almost linear with respect to moderator temperature change from ambient temperature values to near boiling for hydrostatic pressure in the core.

The calculations based on DIF3D¹⁴ suggest fuel coefficient reactivity ranges from -8×10^{-5} to $-1.2 \times 10^{-4} \Delta k/k \text{ } ^\circ\text{C}^{-1}$ for a TRIGA core with a circular grid plate (the UT TRIGA has hexagonal pitch), or -4.5×10^{-5} and $-6.8 \times 10^{-5} \Delta k/k \text{ } ^\circ\text{F}^{-1}$. This is in reasonable agreement with this analysis. The temperature coefficient data is used in TRACE to determine feedback for transient analysis.

3.0 VALIDATION

The neutronics report identifies instrumented elements in core positions B03 and B06 as generating 15.82 kW and 15.39 kW respectively in a 1.1 MW core of 113 elements (based on the MCNP calculations). The UT TRIGA administratively limits power operation to 950 kW, 86.4% of the licensed power level; therefore, the power levels generated in the thermocouple elements at nominal full power operations are 13.66 kW and 13.29 kW. Normal operations occur with a pool (cooling water) temperature of 25°C (77°F) where the limiting core condition assumes 49°C (120°F). Pool level during normal operations is 5.25 m (23.8 ft) above the core while the limiting core condition is 5.25 m (17.2 ft) above the core; hydrostatic pressure is 24.2 psia for normal operations, 21.3 psia for limiting core conditions. A series of calculations using nominal conditions was performed to allow comparison of observed power levels and temperatures to those generated by the TRACE model.

3.1 Steady State

The temperature of the location for each of the three thermocouples in the instrumented fuel elements were calculated using the TRACE model, with the thermocouples in each instrumented fuel element deviating by about 13°C (Table 10). Fuel temperature channel readings were taken from records of operation in December 2018 at 950 kW and compared to TRACE calculations (Table 10). Fuel temperature channel indications were 420°C (FT1) and 334°C (FT2). The highest fuel measuring channel indicated 7.3% above the maximum temperature calculated with MCNP/TRACE data, the lowest IFE channel indicated 10% higher than the lowest indication on the fuel temperature measuring channels. The highest temperature calculated with the TRACE model is about 7% lower than the fuel temperature measuring channel indication, and lowest temperature is about 10% higher.

The difference between the TRACE data from the thermocouples in each IFE is attributed to the axial position of the thermocouples (separated by 1 in. above and below the center thermocouple). There are no records correlating individual thermocouples with specific axial position (although lead wire labeling suggests the center thermocouple may be identifiable). Data calculated at each thermocouple position are therefore included in Table 10.

¹⁴ AFRRRI op cit.

Table 10: Comparison of MCNP/TRACE Calculations and Fuel Temperature Measuring Channel Indications

Element Power (kW)	MCNP/TRACE TC Temps	Fuel Temp Channels	Deviation
13.66	389.03°C	420°C	-7.37%
	387.00°C		-7.86%
	376.03°C		-10.47%
13.29	380.41°C	334°C	13.89%
	378.41°C		13.30%
	367.70°C		10.09%

Comparison of the TRACE calculation and observed data shows reasonably close agreement, with differences that may be partially attributed to IFE fabrication and coupling with the MCNP model. The channels in the fuel meat accommodating the thermocouples reduce the mass of the fuel in the elements slightly, which was not modeled in MCNP. One of the fuel elements was installed in 2018, with the fresh fuel and the gap between fuel and cladding expected to cause elevated temperatures until the fuel has achieved significant burnup. The calculated temperatures are in reasonable agreement with measured data.

3.2 Pulsing Operations

The TRACE calculations were compared to historical data to validate the accuracy of the method used. Historical pulse data (reactivity addition, peak pulse power, and maximum temperature from the fuel temperature measuring channels) was compiled, with incomplete data purged. There is significant scatter in power level (Fig. 6) and temperature (Fig. 7) data with some outliers but the results overall provide a good validation. Pulse records do not include factors with potential to affect pulse characteristics such as initial fuel temperature, pool temperature, or recent operating history that might explain some of the scatter in the data. The TRACE calculations are for individual elements, so peak power level during pulses was distributed across the core for comparison to historical data. Although there is significant scatter and outliers in historical pulse power level data, it is clear that qualitatively the TRACE data agrees well with historical data.

A comparison of peak temperature to historical pulsing data required adjusting the average pulse power to the power generated in the IFE by the ratio of the power in the instrumented fuel elements (identified in the neutronics report) to the average element power. The fuel matrix in IFEs is fabricated with milled channels to accommodate thermocouple leads, and the thermocouples are installed in fuel penetrations extending from the outer surface to near the inner surface of the fuel. Consequently, the volume of the fuel in the IFE is a few percent lower than a standard fuel element. All fuel material specifications in the MCNP model used to calculate power generated in the IFE assumed the same density as standard fuel elements, likely resulting in a higher power generation. It is therefore expected that the peak pulse fuel temperature in the IFEs calculated from MCNP and TRACE (Fig. 7) is slightly higher than historical values. Even with the complications created by MCNP modeling, data scatter, and outliers the TRACE calculations agree well with observed data.

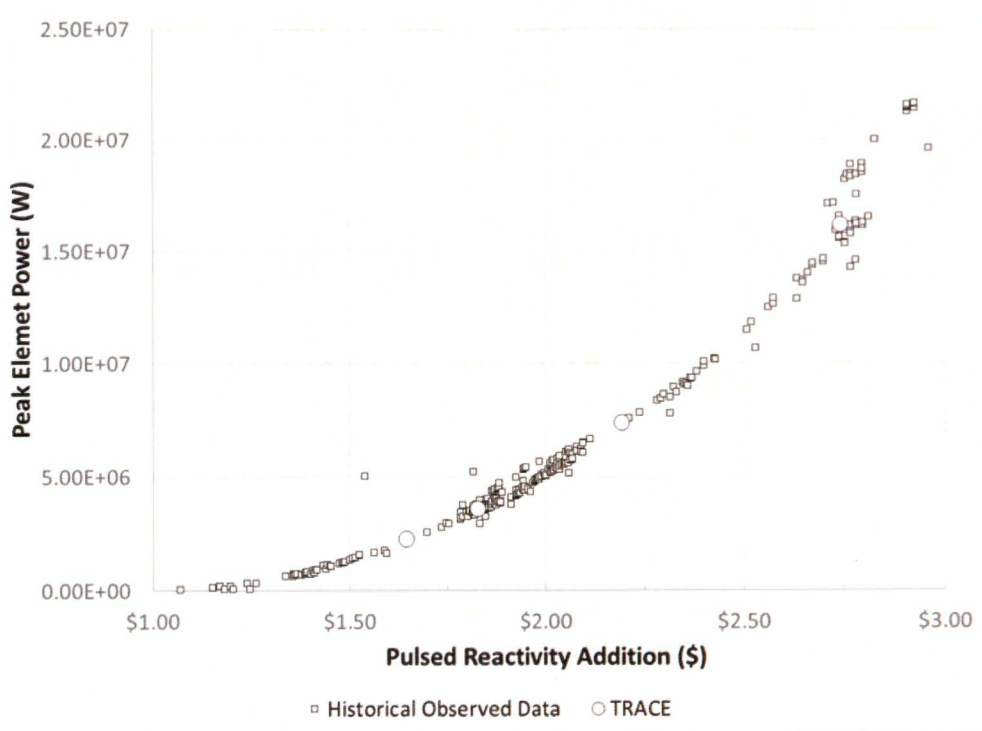


Figure 6: Peak Element Power Level Versus Pulse Reactivity Addition from UT TRACE Calculation Compared to Observed Historical Data

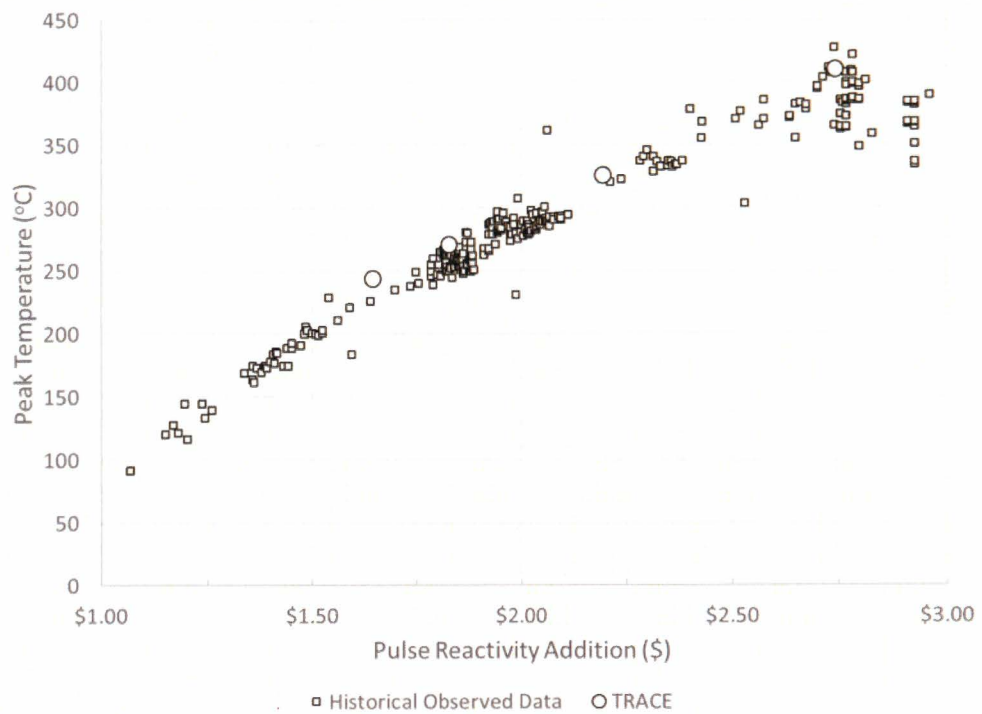


Figure 7: Peak Fuel Temperature Versus Pulse Reactivity Addition from UT TRACE Calculation Compared to Historical Data

3.3 Conclusion

Fuel temperatures indicated by the fuel temperature measuring channels, and power and temperature from historical records of pulsing, were compared to data generated with TRACE calculations. The comparison demonstrates that the TRACE model is capable of predicting thermal hydraulic performance of the UT TRIGA reactor with reasonable accuracy.

4.0 LIMITING CORE CONFIGURATION

4.1 Steady-State Power Level

The neutronic analysis indicates that for a licensed power of 1.1 MW, the maximum power in any element is 22.14 kW with 84 elements. With a maximum potential instrument error of 10%, the maximum power in the hot channel could be as high as 24.34 kW. UT TRIGA hot channel power level in this report is well within TRIGA operating experience, less than reported values for the AFFRI TRIGA reactor (35.3 kW) and the TRIGA conversion reactor at the University of Wisconsin (26.04 kW)¹⁵, and less than the 30 kW value cited in ANL RERTR TM 07 01 (which references the MNCR reactor at 33.2 kW).

To evaluate steady-state performance of the LCC, a series of TRACE calculations were performed for the UT TRIGA for fuel element power levels between 5 kW and 60 kW under limiting core conditions. Temperature dependence of the fuel versus power is shown in Fig. 8 for the hot channel, while the radial and axial distribution across the hot channel are shown in Figs. 9 and 10. Fuel element power at 44.9 kW is found to result in a maximum fuel temperature during steady state operations of 1149.9°C, essentially the maximum safety limit if cladding temperature is less than 500°C. Fuel element power at 36.6 kW results in 948.1°C, approaching the 950°C safety limit if cladding temperature is greater than 500°C.

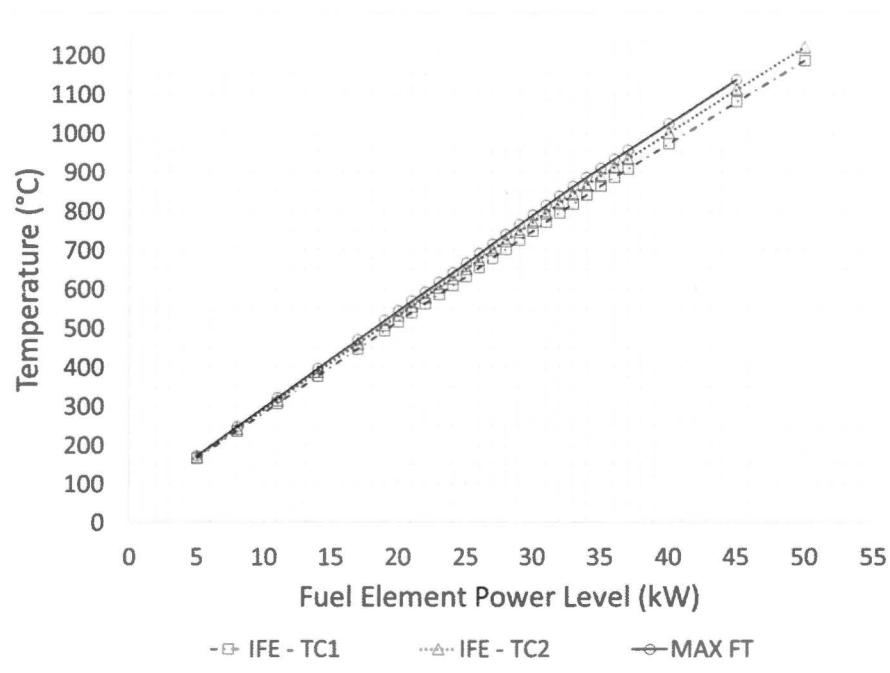


Figure 8: LCC Steady-State Fuel Temperature Versus Fuel Element Power at Each Thermocouple and at the Maximum Fuel Temperature Location

¹⁵ University of Wisconsin LEU Conversion Report (Request for Amendment No. 17 to Facility License No. R-17, 08/25/2008)

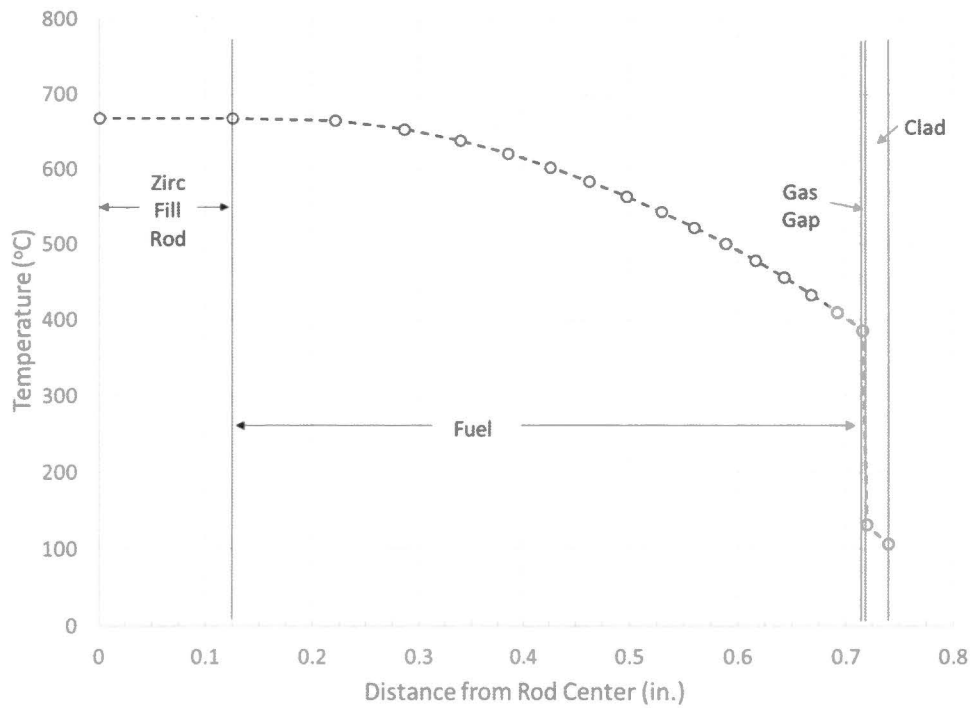


Figure 9: LCC Hot Channel Radial Fuel Temperature Profile at Hottest Axial Position

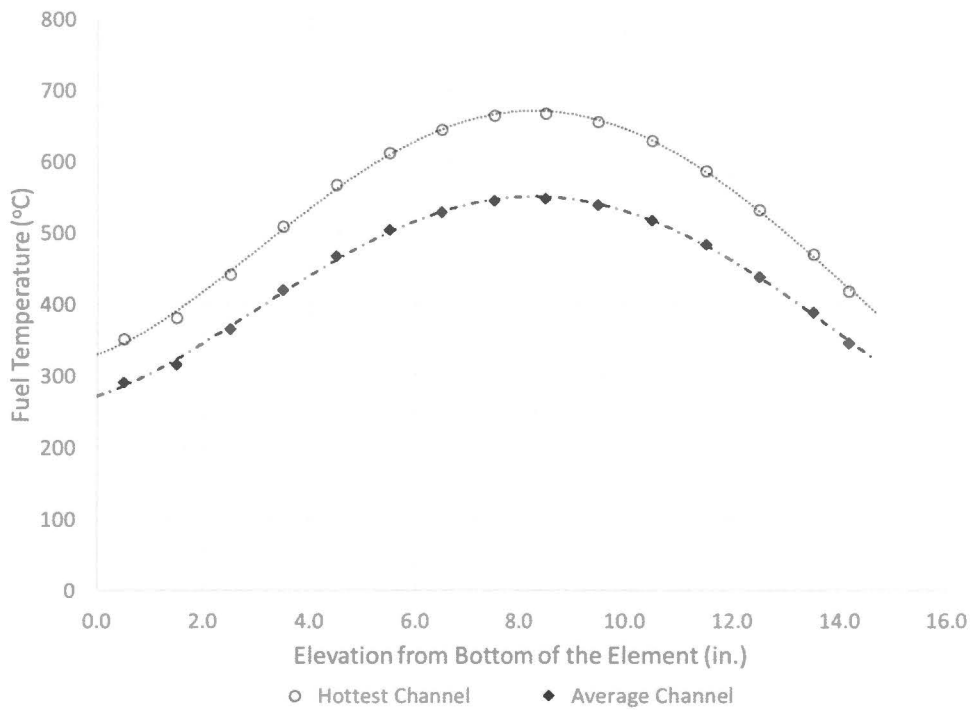


Figure 10: LCC Hot Channel Axial Radial Fuel Temperature Profile

The critical heat flux that leads to burnout is calculated by the Bernath correlation (with variables defined in Table 11):

$$CHF_{BO} = \left[10890 \cdot \frac{D_e}{D_e + D_i} + V \cdot \frac{48}{D_e^{0.6}} \right] \cdot \left(\left[57 \cdot \ln P - 54 \cdot \frac{P}{P + 15} - \frac{V}{4} \right] - T_B \right) F(t_a) \quad \text{Eqn 7}$$

Table 11: Bernath Correlation Variables

Variable	Description	Units	Source
D_e	Hydraulic diameter	ft	Previous formula
D_i	Heater surface diameter	ft	Fuel element diameter
V	Pressure	Psia	Calculated by TRACE
P	Velocity	ft·s ⁻¹	Calculated by TRACE
T_B	Coolant Temperature	°C	Calculated by TRACE

A series of calculations were performed using the Bernath correlation to determine the relationship between element power and the minimum CHF along a rod in limiting core conditions (Fig. 11). The limiting value of 2.0 for CHF occurs at 56 kW generated in the hot channel, in agreement with analysis cited in ANL RERTR TM 07 01. With the UT TRIGA hot channel operating at 24.35, the critical heat flux ratio is 4.69.

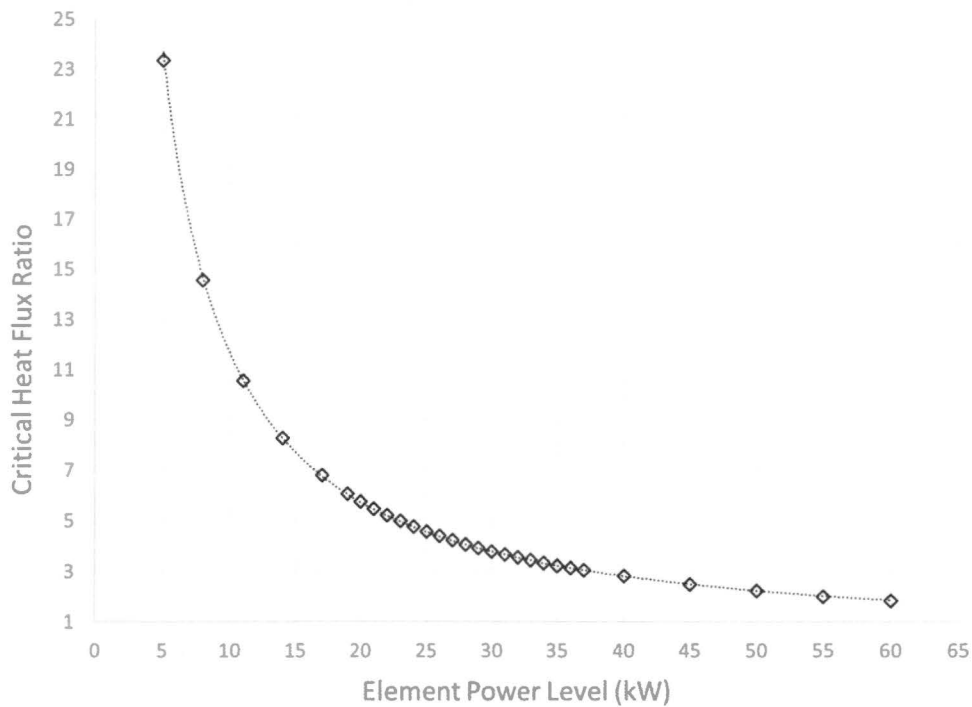


Figure 11: CHF (Bernath Correlation) Versus Fuel Element Power

The critical heat flux ratio varies along the length of the hot channel fuel element at full power as indicated in Fig 12. The minimum CHF is slightly above the center of the section of the fuel element that contains fuel.

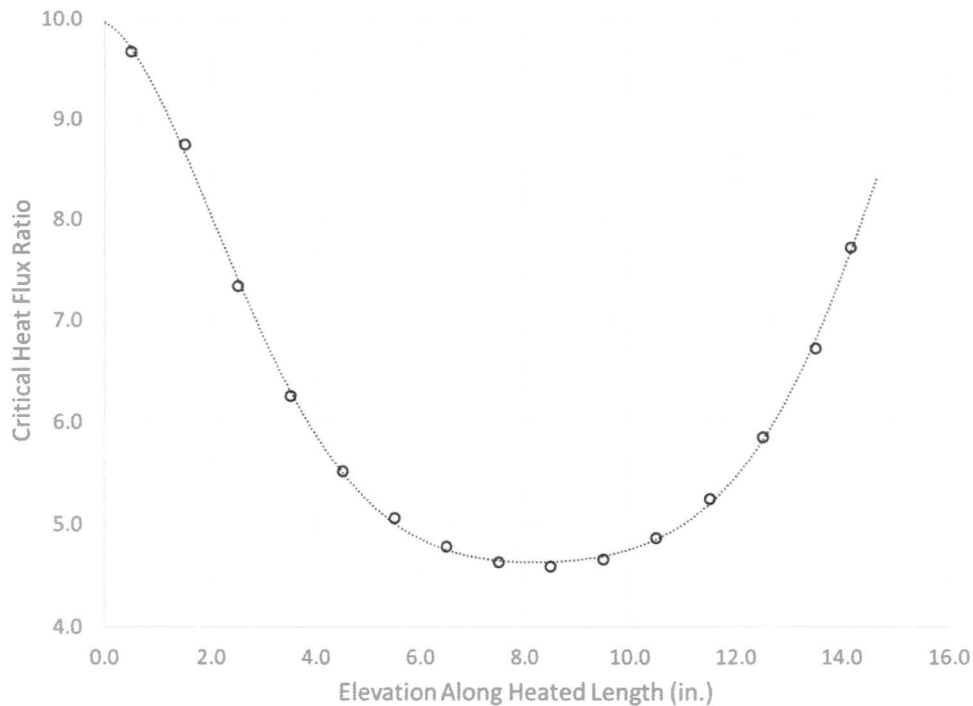


Figure 12: CHFR Hot Channel Axial Values from the Bernath Correlation for UT TRIGA Fuel Element Operating at 24.34 kW

With the hot channel operating at 24.34 kW, the maximum temperature in the core is calculated to be 650°C, approximately 300°C below the 950°C safety limit (68% of the limit). The hot channel element CHFR with power level of 24.34 kW is 4.69 which is significantly above the CHFR limit of 2.0. The power level that would result in a CHFR of 2.0 is at 55 kW which gives significant factor of safety.

4.2 Pulsing Operations

Pulsing reactivity calculations were performed in TRACE for \$3, \$4, \$5, \$6, and \$7 insertions with initial conditions approximating shutdown power levels. The calculations were performed in two steps: (1) using reactivity to calculate time-dependent core power level and (2) using the time/power profile for the second step (with the power of the second step scaled by the hot channel peaking factor). The peak power as a function of pulsed reactivity is shown in Fig. 13, and the time-development of the power pulse for the reactivity insertions in Fig. 14. Note that the \$7 insertion were high enough compared to the other insertions that it was not included so that the remaining data can be shown on a reasonable scale.

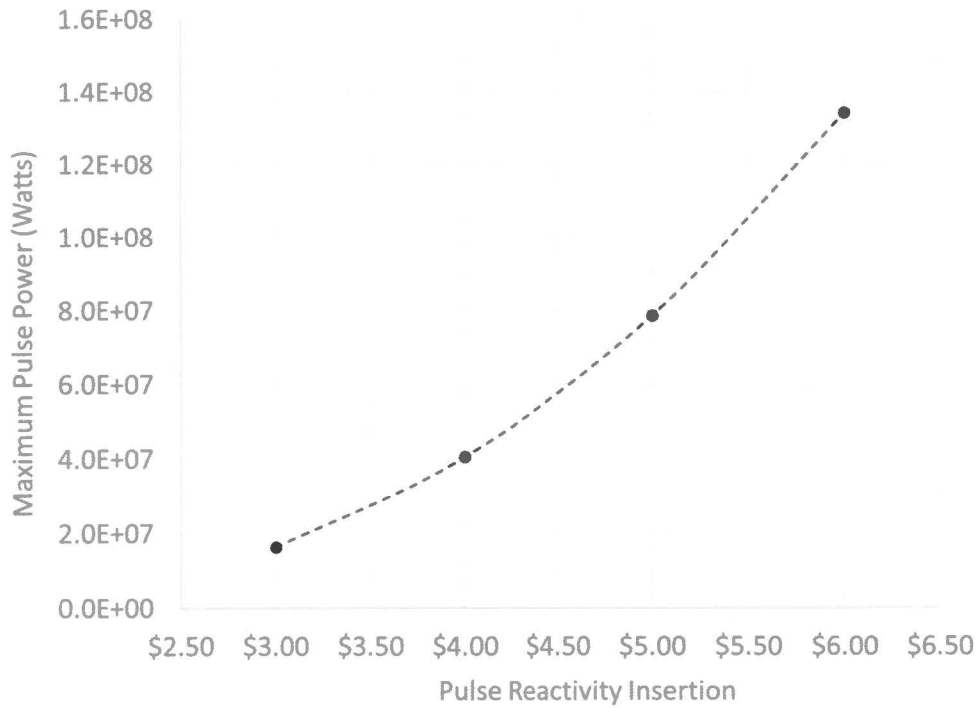


Figure 13: Hot Channel LCC Peak Power Level Versus Reactivity Insertion

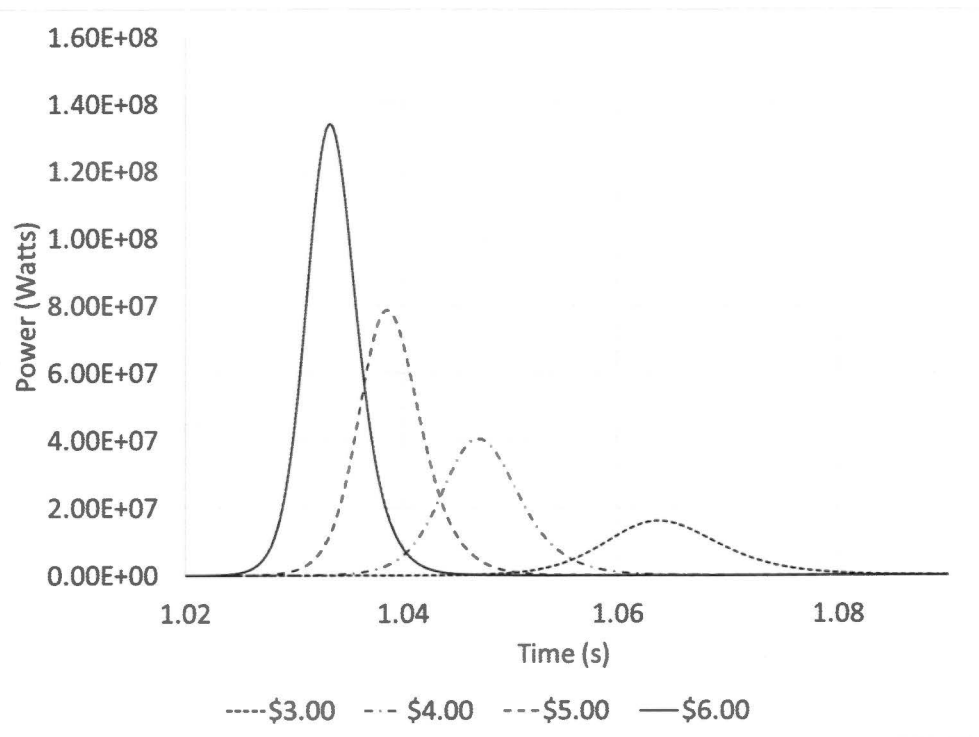


Figure 14: LCC Pulse Power Versus Time for Varying Reactivity Insertions

A \$3 insertion resulted in a peak temperature of 378°C. As shown in Fig. 15, the temperature limit was not exceeded for any reactivity insertions below \$6 (with a 130°C or 16% margin at \$6). The temperature safety limit was not exceeded at a \$7. Time dependent behavior is shown in Fig. 16.

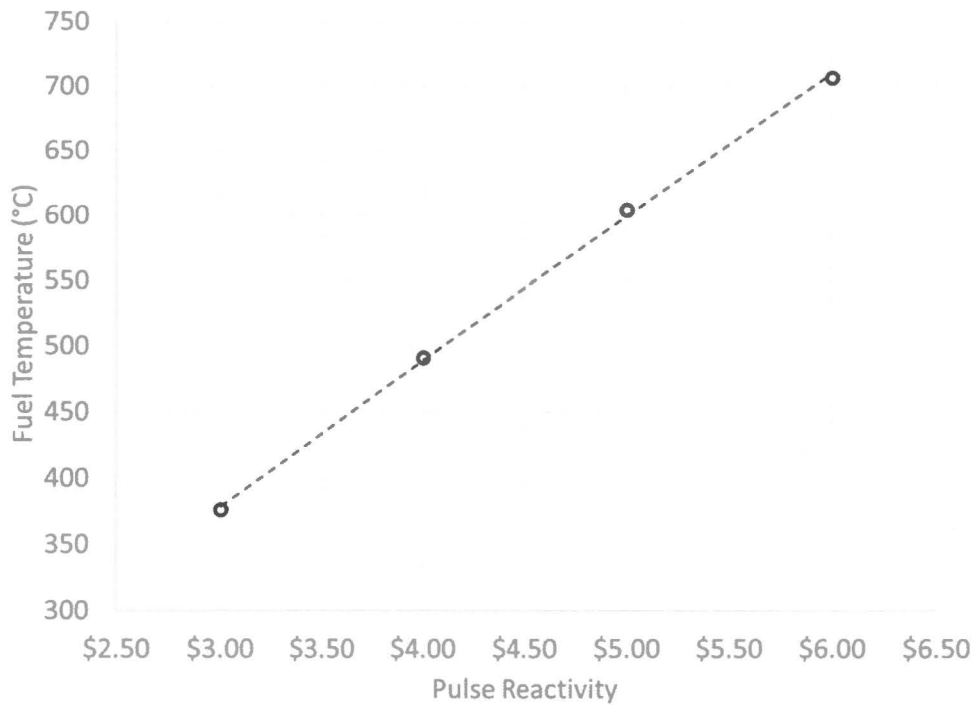


Figure 15: LCC Hot Channel Peak Fuel Temperature Versus Pulse Reactivity Addition

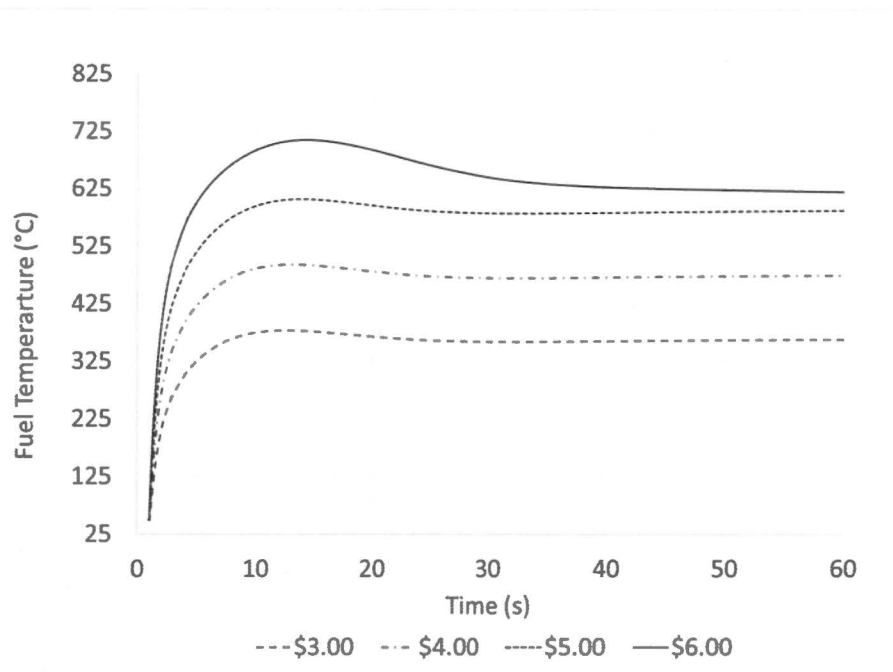


Figure 16: LCC Hot Channel Fuel Temperature Versus Time from Pulse Initiation for Several Pulse Reactivity Additions

The maximum effect of initial conditions at power were evaluated by simulating the reactor operating at the maximum available reactivity with \$3 reserved for the pulsed reactivity addition (core excess at the maximum of \$7). Immediately prior to pulsing operations, the hot channel element was established at 8.25 kW (corresponding to a core power of 43.3 kW). The maximum fuel temperature in the hot channel prior to the pulse was 252 °C, and following the pulsed insertion of \$3, the peak hot channel fuel temperature was 579°C and peak power 74.4 kW (Fig. 17).

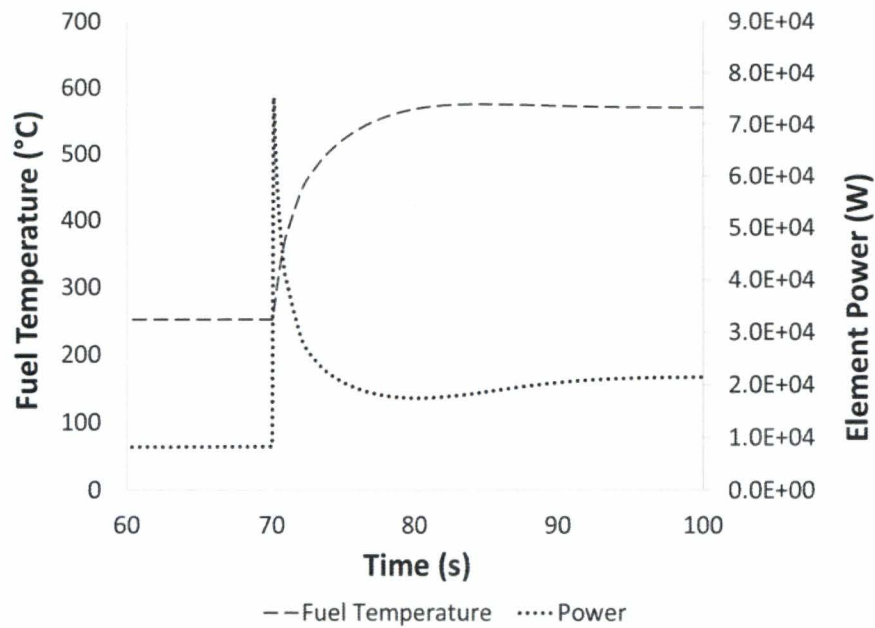


Figure 17: LCC Hot Channel Fuel Temperature and Element Power Versus Time for a \$3 Pulse from Steady-State Operation with Element at an Initial Power of 8.25 kW and Fuel Temperature of 252 °C (Note that pulse was initiated at 70 seconds on the time scale shown)

A maximum pulsed reactivity addition of \$3.00 is adequate to maintain fuel element temperature less than 50% of the limit. Maximum pulsed reactivity addition with the reactor operating at the balance of excess reactivity will not exceed the limiting fuel temperature at any initial achievable power level.

4.3 Continuous Reactivity Addition Transient (Control Rod Withdrawal Event)

Annual measurement of control rod speeds support evaluation of the maximum reactivity addition rate; control rod drive speeds are typically about 30 in. per minute. A set of TRACE calculations were performed to simulate the effect of a continuous control rod withdrawal to the full out position for various integral rod worths. Reactivity addition was modeled based on the fraction of total reactivity added as a function of position, and a constant speed was assumed to determine the fraction of the total integral reactivity added as a function of time for intervals (full in to full out) of 5, 30, 45, 75, 90, 120 and 135 seconds. Scale factors of \$3, \$4, \$5, \$6 and \$7 were applied to each interval. The power and time resulting from this set of calculations was modified with the hot channel peaking factor, and a time dependent power calculation was performed. The characteristic of a 5 second interval are essentially a reactor pulse with a small perturbation on the pulse-tail. Power, temperature, and reactivity characteristics for a reactivity addition to \$3 over 45 seconds is displayed in Figs. 18 and 19. The CHF_R (using the Bernath correlation) was calculated as a minimum of 2.41 for the \$7 reactivity additions to a minimum of 5.76 for a \$3 addition, both at 135 seconds (2.25 minutes) for full reactivity addition.

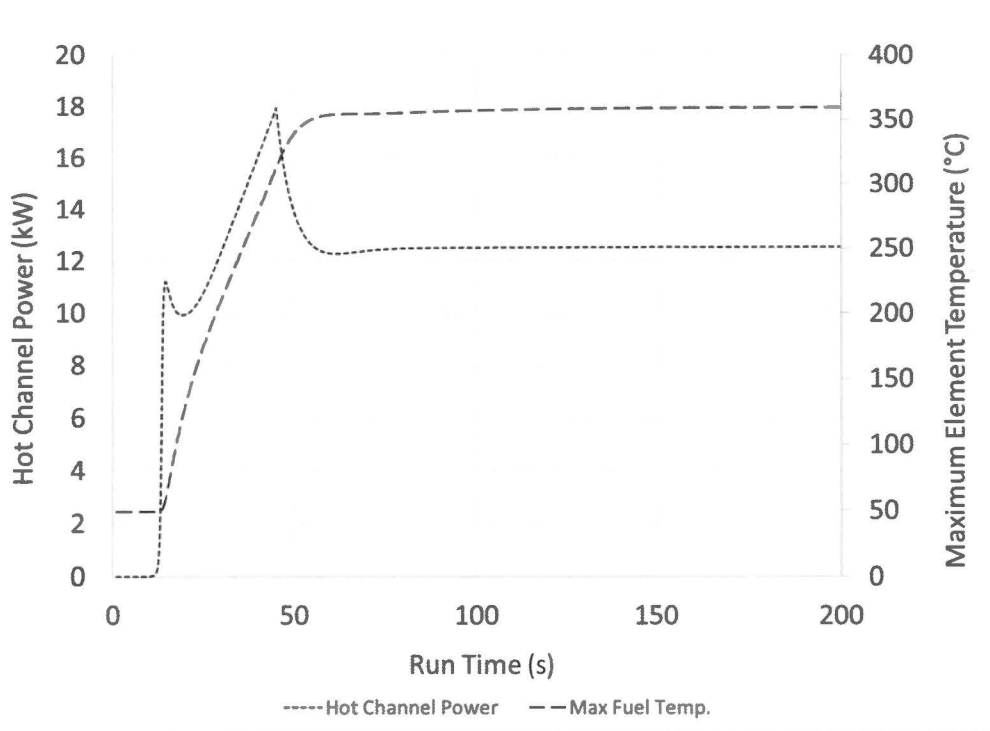


Figure 18: Hot Channel Power and Maximum Fuel Temperature Versus Run Time for a \$3 Reactivity Addition in 45 Seconds

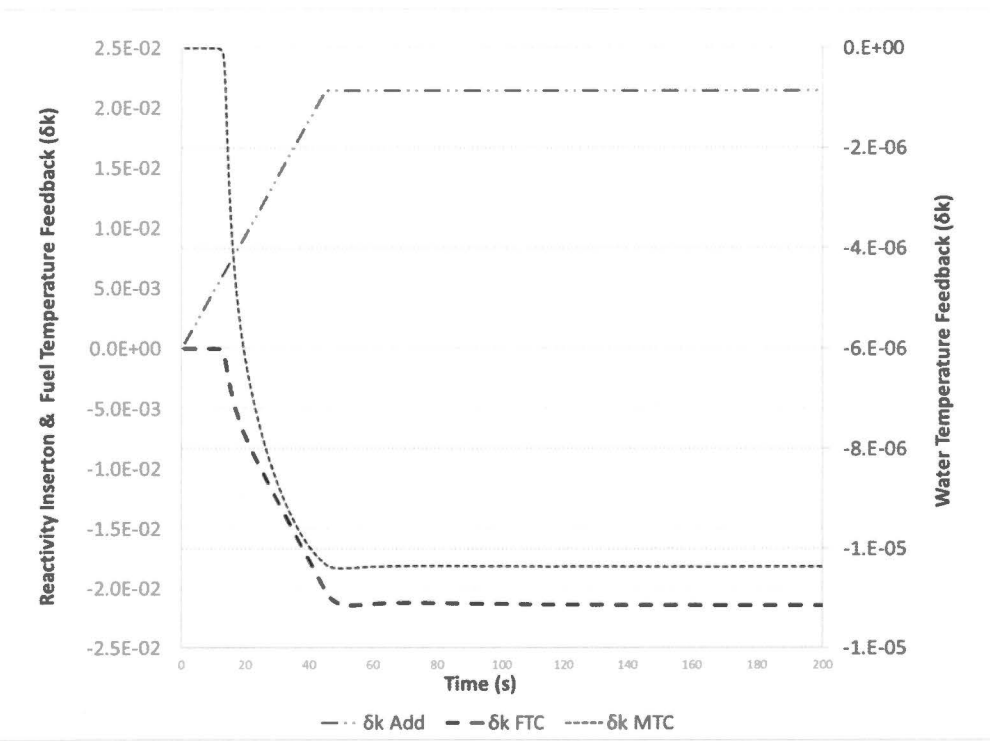


Figure 19: Reactivity Addition, Fuel Temperature Reactivity Feedback, and Moderator Temperature Reactivity Feedback Reactivity Versus Time for a Continuous Reactivity Addition for \$3 in 45 Seconds

The maximum fuel temperature at \$3 and \$4 reactivity additions (748°C) did not vary significantly at any interval. The maximum fuel temperature for the \$5 reactivity addition was 925°C for intervals from 30 seconds to 90 seconds and exceeded 950°C for intervals greater than 90 seconds (as well as all \$6 and \$7 reactivity additions). Maximum fuel temperature values at \$4.5 and \$4.75 at 135 second intervals were tested and found to be 791°C and 835°C, respectively.

Power level response versus time is illustrated in Figs. 20 and 21 for \$3 and \$7 insertions that occur over a range of intervals. As the interval time for the reactivity addition increases, the maximum power over the interval decreases.

Therefore, it was concluded that continuous complete withdrawal of control rods with an integral worth less than \$4.75 at a control rod drive speed less than 0.11 in. per second (6.7 in. per minute) is adequate to maintain fuel temperature less than the maximum fuel temperature limit. Continuous full withdrawal of control rods with an integral worth less than \$5 and a control rod drive speed less than 0.17 in. per second (10 in. per minute) approaches but remains below the maximum fuel temperature limit.

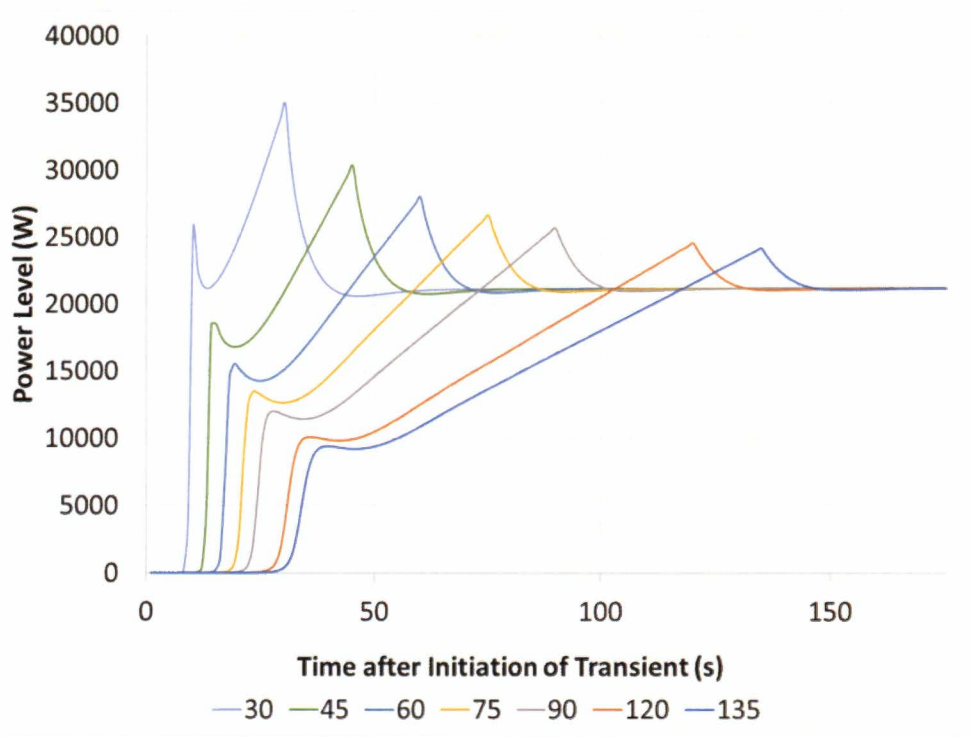


Figure 20: Power Level Versus Time After Initiation of Transient for a Continuous Rod Withdrawal of \$3 in Reactivity

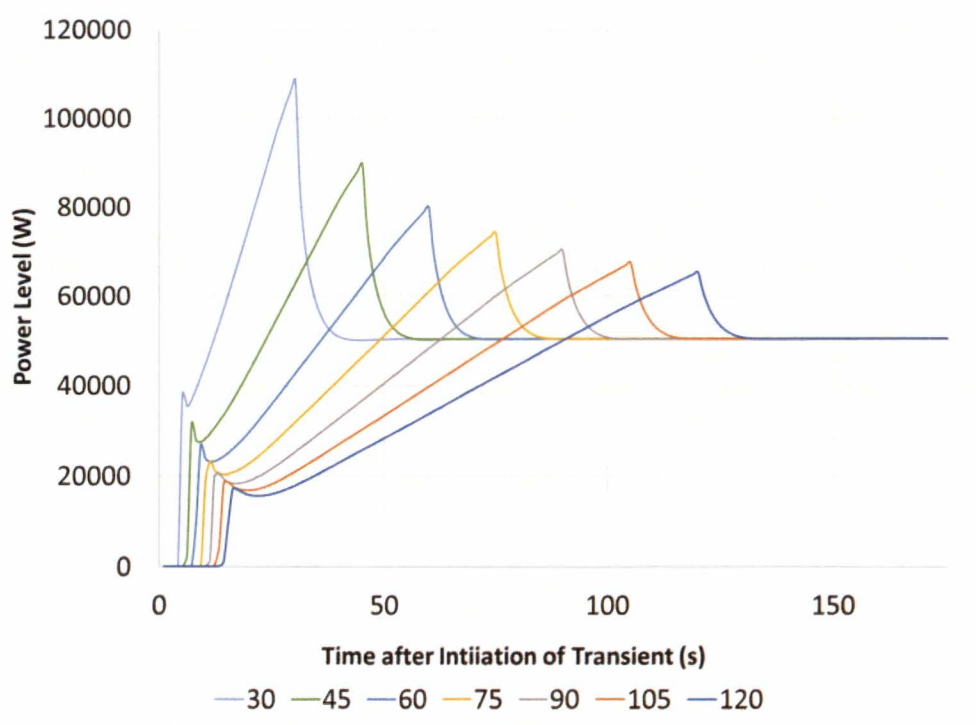


Figure 21: Power Level Versus Time After Initiation of Transient for a Continuous Rod Withdrawal of 7\$ in Reactivity

4.4 LOCA Analysis

The LOCA analysis is initiated with a steady-state TRACE calculation to establish initial conditions, operating at 25 kW until all temperatures are stable. A TRACE restart case was initiated as a transient calculation following the initial calculation, with fission and fission product power decay in time established using the method of ANSI/ANS-5.1-2014, Decay Heat Power in Light Water Reactors (as described). Four cases were calculated (table 12) using four intervals between shutdown and instantaneous replacement of water cooling with air cooling. The time-dependent behavior is shown in Fig. 22 over four hours following shutdown.

DELAY FOR AIR COOLING (s)	MAXIMUM TEMPERATURE (°C)
1	709
60	699
600	663
1200	637

In a rational scenario, an automatic shutdown will be initiated before the core is voided. Drain down of pool water under the most exaggerated conditions will require on the order of 10 to 20 minutes before water cooling is secured. A 10-minute delay will result in a maximum temperature of 663°C, and a 20-minute delay will result in a maximum temperature of 637°C.

There are other practical considerations not considered in modeling that make the analysis conservative in a LOCA event. A drain-down through the beam ports (the only path for flow) will not drain below the core, and some lower portion of the fuel elements will remain in a water environment to provide heat with conduction through the stainless-steel cladding. The air cooling will occur in extremely humid conditions, increasing heat removal capability.

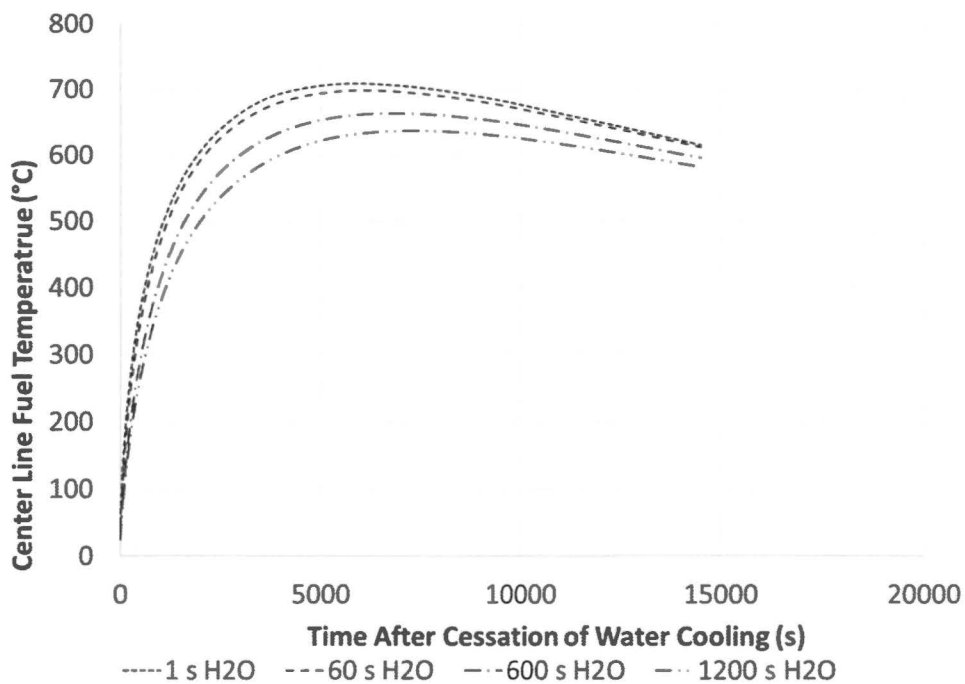


Figure 22: Maximum Post LOCA Temperatures for a 25 kW Element Versus Time Following a LOCA Event (shown for a variety of delay times for air cooling)

Analysis of fuel performance during a LOCA for the AFFRI reactor predicated on 72 hours of full power per week indicates a maximum fuel temperature of about 550°C if there is no delay before water displacement and about 475°C assuming a 15-minute delay. The UT analysis assumes equilibrium steady state analysis, about 2.3 times the power history of the AFFRI reactor, generating more decay heat.

In the event of the LOCA, fuel temperature is calculated to rise to 709°C, 75% of the limiting temperature and a margin of 241°C to the limiting temperature, for a minimal 1 second delay between reactor shutdown and displacement of water. The LCC is adequate maintain fuel integrity unchallenged by temperature in a LOCA.

5.0 SUMMARY AND CONCLUSION

A thermal-hydraulics calculation using TRACE linked to a neutronics calculation using MCNP 6.2 was performed to verify the safety margins available in operation of the UT TRIGA reactor limiting core configuration. There are two limits that ensure fuel integrity during steady state operations and one for pulsing. During steady-state operations a fuel temperature limit of 950°C and a CHF limit of 2.0 applies. During pulsing operations, a fuel temperature limit of 830°C applies.

With a limiting core configuration producing 24.3 kW in the hottest element in the core, analysis shows that the CHF is greater than 4, and fuel temperature is 650°C. Therefore, the limiting core configuration does not exceed limits during steady-state operations at 1.21 MW with a large margin of safety available.

In pulsing operations to \$3 from non-power conditions, the maximum fuel temperature is calculated to be 378°C. When pulsing at power, from the maximum power level available with \$3 reserved for pulsing, the

maximum fuel temperature is calculated to be 579°C. Both of these temperatures are well below the limit. Therefore, a \$3 pulsing limit is adequate to assure the safety limit is met by a large margin.

The maximum fuel temperature from a continuous reactivity addition event to less than \$4.75 at any reactivity addition rate will not exceed 835°C. Therefore, an integral control rod worth less than \$4.75 is adequate to limit fuel temperature in a continuous rod withdrawal event to the safety limit with a substantial margin. If integral control rod worth is \$5 in the event, temperature will not exceed the safety limit with a minimal margin as long as control rod speed does not exceed approximately 3 times the normal control rod speed.

A loss of coolant accident after continuous full power operations to steady-state conditions will not result in fuel temperature greater than 709°C with air cooling (with the cooling delayed by 1 second). Therefore, 1.21 MW operations ensures cooling is adequate for fuel integrity in a loss of coolant accident by a large margin.